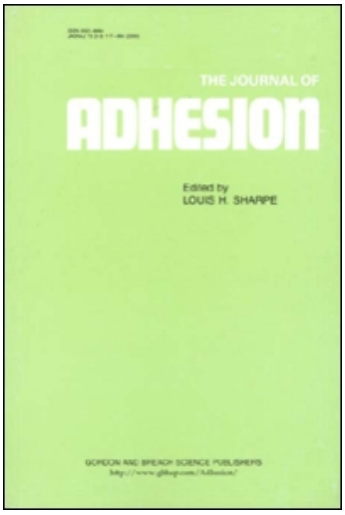

The Journal of Adhesion
Publication details, including instructions for authors and subscription information:
http://www.informaworld.com/smpp/title~content=t713453635

Temperature Effects on Interdiffusion at Glassy/Rubbery Interfaces

E. Jabbari[ab]; N. A. Peppas[a]
[a] School of Chemical Engineering, Purdue University, West Lafayette, IN, U.S.A. [b] North American Division, Monsanto Company, St. Louis, MO, U.S.A.

To cite this Article Jabbari, E. and Peppas, N. A.(1993) 'Temperature Effects on Interdiffusion at Glassy/Rubbery Interfaces', The Journal of Adhesion, 43: 1, 101 — 119
To link to this Article: DOI: 10.1080/00218469308026591
URL: http://dx.doi.org/10.1080/00218469308026591

J. Adhesion, 1993, Vol. 43, pp. 101–119
Reprints available directly from the publisher
Photocopying permitted by license only

Printed in the United States of America

Temperature Effects on Interdiffusion at Glassy/Rubbery Interfaces*

E. JABBARI† and N. A. PEPPAS**

School of Chemical Engineering, Purdue University, West Lafayette, IN 47907-1283, U.S.A.

(Received March 11, 1993; in final form July 8, 1993)

Attenuated total reflection infrared spectroscopy was used to measure interdiffusion at a model glassy/rubbery interface consisting of polystyrene (PS) below its glass transition temperature in contact with poly(vinyl methyl ether) (PVME). PVME swelled PS at temperatures ranging from 60 to 95°C, corresponding to 41 to 6°C below the glass transition of PS. This swelling was confirmed with dynamic mechanical analysis using glassy crosslinked PS in contact with PVME. The swelling process was characterized by an interfacial velocity as the PVME swelled PS. The relaxation time for the swelling process was determined from the interface velocity as a function of temperature and the results indicated that the swelling process is controlled by the relaxation time of the slowly diffusing component (PS). The relaxation time ranged from 141 min at 60°C to 16.8 s at 95°C. The activation energy for the relaxation of the PS matrix was determined as 40.9 ± 2.6 kcal/mol using the Arrhenius expression, in good agreement with values reported in the literature for the β relaxation of PS which are in the range of 35–40 kcal/mol.

KEY WORDS infrared spectroscopy; glassy polystyrene; poly(vinyl methyl ether); swelling; temperature effect; interface velocity; relaxation time; activation energy; adhesion of polymers.

1. INTRODUCTION

In general, adhesion at polymer-polymer interfaces affects the mechanical properties of polymers near these interfaces.[1] This process influences, in turn, various phenomena such as welding of polymer interfaces and lamination of composites.

The implications of this adhesion phenomenon in a wide range of applications is quite evident. For example, in encapsulation of microelectronic devices, a multilayer chip consisting of many conductor layers stacked together with dielectric polyimide layers is covered with a passivation layer, which is also a polyimide, to stop the intrusion of alpha rays. Next, the chip is mounted on a board and is encapsulated with a layer of epoxy to stop moisture diffusion into the chip. Polyimide-polyimide and polyimide-epoxy adhesion are crucial to the encapsulation of microelectronic

*Presented at the Fifteenth Annual Meeting of The Adhesion Society, Inc., Hilton Head Island, South Carolina, U.S.A., February 17–19, 1992.

**Corresponding author.

†Present address: North American Division, Monsanto Company, 800 N. Lindbergh Blvd., St. Louis, MO 63167, U.S.A.

devices. Previous results[2] show that polyimide-polyimide adhesion of a solution-cast polymer film to a previously-deposited and cured underlayer can be improved by first swelling the polymer underlayer, thereby increasing chain interpenetration across the interface.

Another recent application of polymer adhesion is in copolymer-enhanced adhesion for polymer composites.[3] Polymer composites have complementary mechanical properties compared with homopolymers but they suffer from poor adhesion at the polymer-polymer interface. The fracture energy of a polymer-polymer interface can be improved by an order of magnitude by addition of an A/B block copolymer consisting of blocks with molecular weights above the entanglement molecular weight. This phase acts as an interfacial agent between the homopolymers A and B.

Similarly, in packaging of food products, an oxygen barrier polymer layer is sandwiched between two polyolefin moisture barrier layers. The performance of the laminated structure is dominated by the adhesion and bond strength between the barrier layers to oxygen and moisture. Polymer-polymer adhesion is also important in autoadhesion of polymers, such as in tires, where adhesion is required at the compound-compound interface.

Microscopic adhesion is related to the sum of all the intermolecular interactions at the interface and depends exclusively on the interfacial characteristics.[4] On the other hand, macroscopic adhesion is related to the dissipative processes at the interface and is affected by specimen geometry and measurement technique. The adhesive strength of a bond is the sum of the microscopic as well as macroscopic interactions at the interface.

Polymer/polymer adhesion may be interpreted by the adsorption theory,[5] wetting theory,[6] electrostatic theory,[7] chemical healing,[8] diffusion theory,[9,10] fracture theory,[1] kinetic theory,[11] and mechanical interlocking.[12] Of these theories, the diffusion theory of Voyutskii[9] is of particular interest to us. After intimate contact is established between two polymer films, adhesion takes place by interdiffusion of polymer segments across the interface. The extent of interdiffusion and chain interpenetration depends on the compatibility between the two polymers. For incompatible polymers, the interface thickness is controlled by the surface free energy of the components and is of the order of angstroms.[13] On the other hand, for compatible polymers the surface free energy plays an important role in the initial phase of wetting, but the interface thickness is controlled by the Flory-Huggins interaction parameter between the polymers[14] and is of the order of microns.[15]

A number of techniques have been developed for measuring interdiffusion at polymer-polymer interfaces. These include small angle neutron scattering,[16] X-ray reflectometry,[17] forward recoil spectrometry,[18] transmission electron microscopy,[19] Raman scattering,[20] and infrared microdensitometry.[21] These techniques have provided uniequivocal evidence for interdiffusion at polymer-polymer interfaces and the diffusion theory of adhesion.

The polymer pair polystyrene, henceforth designated by PS, and poly(vinyl methyl ether), henceforth designated by PVME, with very dissimilar properties, has been used extensively as a model to study adhesion at glassy and rubbery interfaces, with applications to rubber-toughened polymer composites. These results

indicate that when a glassy and rubbery polymer come into intimate contact, the rubbery polymer swells the glassy polymer matrix. In lamination of composites, the polymer bilayer is annealed for a specified period of time at temperatures near the glass transition temperature of the two polymers to improve their interfacial adhesion. The temperature and duration of the annealing process directly affects the interfacial thickness and the strength of the glassy/rubbery interface.

Results from Sauer and Walsh[22] and our laboratory[23] have shown that for polymer interfaces with dissimilar properties, after intimate contact is established between two polymers, the faster-diffusing component swells the slower-diffusing component prior to interdiffusion across the interface for below and above the T_g of the slow-diffusing component. These results were obtained using a polymer pair consisting of PS as the slowly-diffusing component with T_g of 101°C and PVME as the fast-diffusing component with T_g of −27°C. The temperature range of the experiment was from 85 to 105°C, spanning temperatures below and above the T_g of PS.

Despite these studies, the importance of temperature on polymer/polymer diffusion has not been described in detail. Therefore, the objective of this work was to investigate experimentally the effect of temperature below the T_g of the glassy polymer on the interfacial thickness of the glassy/rubbery interface using the model pair PS and PVME. A technique based on attenuated total reflection infrared spectroscopy, henceforth designated as ATR-FTIR, is used for quantitative analysis of interdiffusion at glassy/rubbery interfaces.

2. EXPERIMENTAL

Polystyrene was obtained from Pressure Chemical Co. (Pittsburgh, PA) as a primary standard with number average molecular weight, $\overline{M}_n$, of 1.0×10^5 and polydispersity index, PI, of 1.06. The PVME was obtained from Scientific Polymer Products (Ontario, NY) as a secondary standard with $\overline{M}_n$ of 4.7×10^4 and PI of 2.10. Gel permeation chromatography was carried out in a chromatograph (model 6000A, Waters Associates, Milford, MA) using tetrahydrofuran as the mobile phase and μStyragel® columns with 10^6, 10^5, 10^4, 10^3 Å pore sizes and 1 mL/min flow rate. It indicated that no additives were present in the polymer. The PS and PVME samples had T_g of 101°C and −27°C, respectively, measured by differential scanning calorimetry (DSC 2910, TA Instruments, Wilmington, DE). A thermogravimetric analyzer (Hi-Res TGA 2950, TA Instruments, Wilmington, DE) was used to study the degradation behavior of PVME and its blends with polystyrene.

An FTIR spectrometer (Nicolet 800, Madison, WI) with the ATR accessory (Connecticut Instruments, Boston, MA) were used for the interdiffusion studies in the configuration shown in Figure 1. The ATR crystals were zinc selenide (ZnSe) or germanium (Ge) with 5 cm length, 1 cm width, and 2 mm thickness. A polystyrene film was cast on a germanium (Ge) or zinc selenide (ZnSe) ATR crystal with a spin coater (model 1-EC101D-R485, Photo-Resist Spinners, Garland, TX) from p-xylene solution at 250 rpm. The PS film was dried in a controlled atmosphere at 25°C for at least 24 h, then *in vacuo* at 25°C for 24 h, followed by *in vacuo* at 115°C for 1 h to remove any residual solvent in the film. The film was then annealed

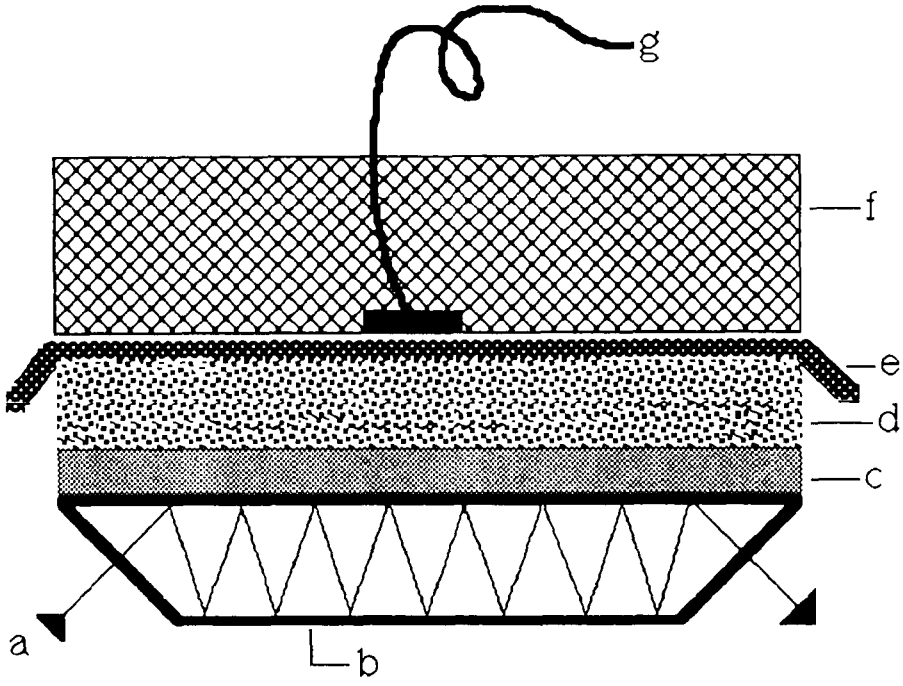

FIGURE 1 ATR assembly for *in situ* measurement of polymer/polymer interdiffusion. a: infrared light beam; b: ATR crystal; c: PS layer; d: PVME layer; e: aluminum foil; f: heating unit; g: thermocouple.

at 115°C for at least 12 h to remove solvent and minimize molecular orientation resulting from the spinning process. The thickness and surface roughness of the PS film were measured using a profilometer (alpha-step 200, Tencor Instruments, Mountain View, CA).

The PVME was cast directly on the PS film from isobutanol solution using the spin coater, as previously described. The PVME film was dried at 25°C for 24 h and then *in vacuo* at room temperature for 24 h to remove residual water. Since the T_g of PVME is below room temperature, further drying at higher temperatures was not necessary. For the experiments with Ge crystals, the PS and PVME films were cast from a 1 wt% p-xylene and 5 wt% isobutanol solutions, respectively. For the experiments with ZnSe crystals, the PS and PVME films were cast from 5 wt% p-xylene and 10 wt% isobutanol solutions, respectively.

The thickness of the PVME film was measured by casting a PVME film on glass microscope slide, with the same dimensions as the ATR crystal, under the same spinning conditions. The film was dried at 25°C for 24 h and then *in vacuo* at room temperature for 24 h to remove residual water. The glass slide was weighed before and after the PVME film was cast. The thickness of the PVME film was determined from the weight of PVME and the dimensions of the glass slide. The thickness of the PVME film cast from 5 and 10 wt% isobutanol solution was 3.1 μm and 6.6 μm, which was the average of four samples.

The use of ATR-FTIR for interdiffusion studies at polymer-polymer interfaces was described by us before.[23] Briefly, the infrared beam enters the ATR crystal from one of the side faces. If the refractive index of the crystal is higher than the PS and the incident angle of the beam is higher than a critical angle then the infrared beam is totally reflected at the crystal/PS interface and the beam travels inside the crystal and exits from the other side face. However, at the crystal/polymer interface,[24] a small fraction of the beam penetrates into the PS layer and is absorbed by PS. The fraction of the beam which is absorbed gives rise to absorption bands in the ATR spectrum which can be used to monitor the concentration of each component within the penetration depth in the polymer layer.

In a typical experiment, a PS film was cast by spin coating from p-xylene solution on a Ge or ZnSe crystal. The PS film was dried in a controlled atmosphere to remove any residual solvent. The PVME was spin cast directly on the PS film from isobutanol solution to ensure good adhesion and molecular contact at the PS/PVME interface. The assembly consisting of the ATR crystal, the two polymer films, the aluminum foil (see Fig. 1), and the heating unit was heated to the desired interdiffusion temperature and the ATR-FTIR spectrum was collected *in situ* with 128 averaged scans and a resolution of 4 cm^{-1}. The end-face angle of the ATR crystal and the optical angle of the infrared beam were 45°.

Dynamic mechanical analysis (DMA model 983, TA Instruments, Wilmington, DE) was used to examine the relaxation spectrum, and the shear loss and storage moduli, of crosslinked polystyrene in contact with PVME. The shape of the samples tested was rectangular. They were 8 mm in length, 7 mm in width, and 0.6 mm in thickness. Since the samples were relatively thin, low mass vertical clamps were used and the experiment was conducted at a fixed frequency of 1 Hz.

Crosslinked PS was synthesized by bulk polymerization of styrene (Aldrich Chemicals Co., Milwaukee, WI) distilled under reduced pressure (5 mm Hg) at 30°C to remove the inhibitor, 4-tert-butylcatechol. Thermal polymerization was carried out and the crosslinking agent divinylbenzene (DVB, Aldrich Chemicals Co., Milwaukee, WI) was used without further purification. In a typical experiment, crosslinking reactions were run in Petri dishes at a nominal crosslinking ratio, X, of 0.005 mol DVB/mol styrene, corresponding to 28 mg of DVB in 5 mL styrene. The mixture was allowed to react for 24 h at 115°C. The thickness of the crosslinked PS film was 0.6 mm. A thin film of PVME was spin cast on the crosslinked PS from a 10% isobutanol solution at 250 rpm. The PVME film was dried at 25°C for 24 h and then *in vacuo* at room temperature for 24 h to remove residual solvent.

3. RESULTS

ATR-FTIR was used to measure interdiffusion in a PS and PVME compatible pair below and above the glass transition of PS (Fig. 1). The PS film was cast by spin coating on Ge and ZnSe crystals. The thickness of the PS film was measured as a function of distance along the crystal length from the center and is reported in Figure 2. The PS film thicknesses cast from 1 and 5 wt% p-xylene solutions were 90 and 700 nm, respectively. The surface roughness of the PS films was less than 20

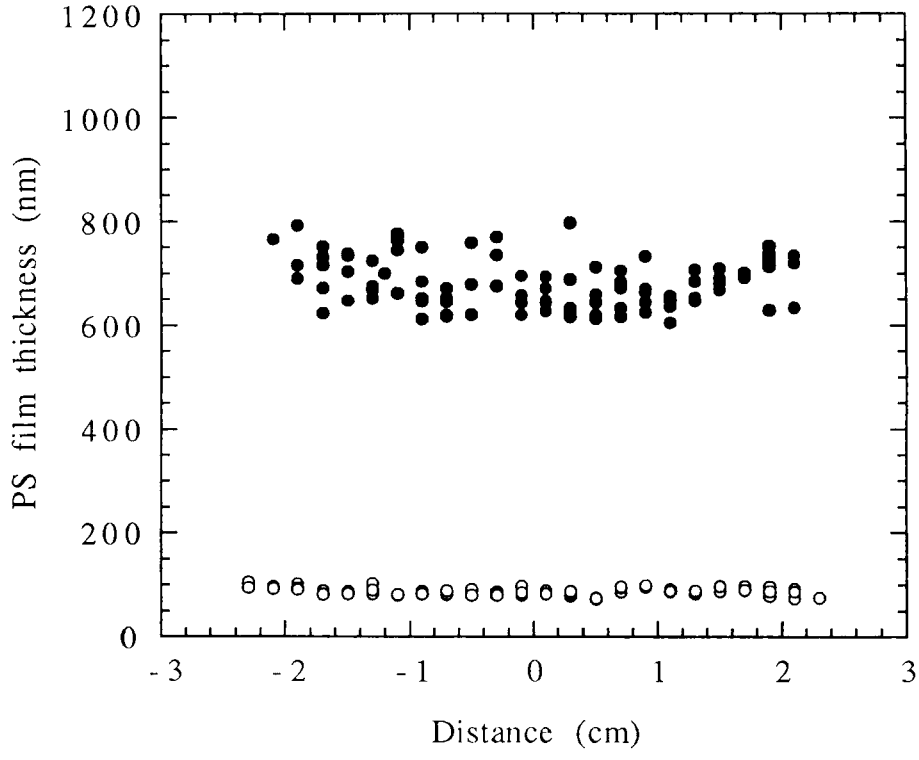

FIGURE 2 Thickness of the PS film on a Ge crystal. The PS with molecular weight, $\overline{M_n}$, of 1.0×10^5 and polydispersity index of 1.06 was spin cast at 250 rpm from a 1 wt% (○) or a 5 wt% (●) p-xylene solution.

nm, measured with a profilometer. The surface roughness was the average of 10 scans over a 80 μm horizontal distance.[23] The thicknesses of the PVME films cast from 5 and 10 wt% isobutanol solution were 3.1 and 6.6 μm, respectively.

PVME is unstable in oxygen atmosphere as reported by Park *et al.*[25] A thermogravimetric analyzer (TGA) was used to monitor the stability of PVME as a function of temperature. According to TGA results, the PVME is stable for at least 24 h at 95°C with increased stability at lower temperatures. Yang *et al.*[26] have investigated the phase diagram of PS with $\overline{M_n}$ of 1.0×10^5 and PI of 1.05 and PVME with $\overline{M_n}$ of 4.7×10^4 and PI of 2.13, samples which have the same molecular weight and polydispersity as our samples, and they report a lower critical solution temperature (LCST) of 125°C. Therefore, the temperature range of 60 to 95°C used in our experiments is well below the LCST of this blend.

The ATR-FTIR spectrum of PS and PVME in the high frequency region and the assignment of each absorption band have been discussed elsewhere.[23] Figure 3 shows the ATR-FTIR spectrum of a 50/50 w/w PS/PVME in the high frequency region from 2700 to 3200 cm^{-1}. The seven absorption bands of PS with peak locations at 2850, 2930, 3000, 3030, 3060, 3085, and 3105 cm^{-1} and the four bands of

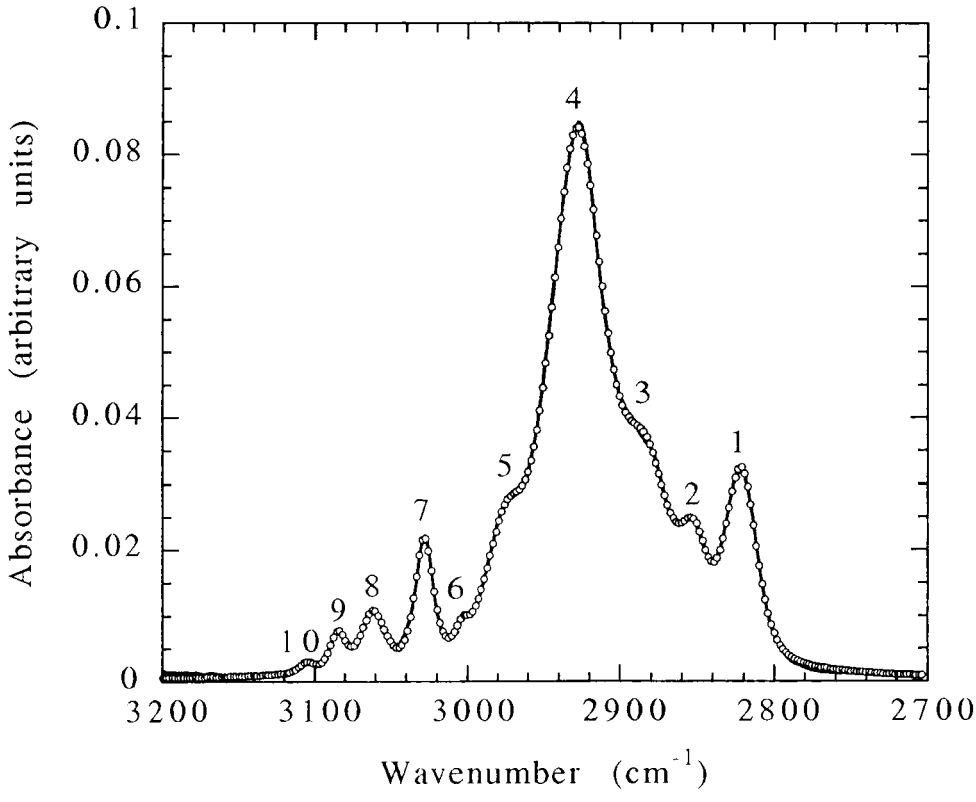

FIGURE 3 ATR-FTIR spectrum of a 50/50 w/w PS/PVME mixture in the high frequency region. The open circles and the continuous line represent the original and the convoluted spectrum, respectively. The best fit was obtained with a 50% Lorentzian and 50% Gaussian distribution. The peak frequencies 1 through 10 are 2820, 2850, 2880, 2930, 2975, 3000, 3030, 3060, 3085, and 3105 cm^{-1}, respectively.

PVME with peak locations at 2820, 2880, 2930, and 2975 cm^{-1} combine to give ten bands with the PS and PVME bands at 2930 cm^{-1} superimposed.

No significant change in the peak position or the shape of the bands was observed with temperature or composition.

The PVME band at 2820 cm^{-1} and the PS bands at 2850 and 3030 cm^{-1} were used for quantitative analysis of the PS/PVME spectra. The intensity of these three peaks was most sensitive to changes in PS/PVME blend composition. For quantitative analysis, the PS/PVME spectrum was deconvoluted to relate the area under the three peaks to PS and PVME mole fractions. The deconvolution program uses the Levenberg-Marquardt fitting routine to fit the experimental convoluted absorbance data to a set of calculated Gaussian or Lorentzian peaks.[23] Figures 3 and 4 show the comparison of actual and deconvoluted ATR-FTIR spectrum for a 50/50 w/w PS/PVME mixture. The best fit was obtained with a 50% Lorentzian and 50% Gaussian peak composition.

To relate the molar fraction of PVME to the relative absorbance of PVME and

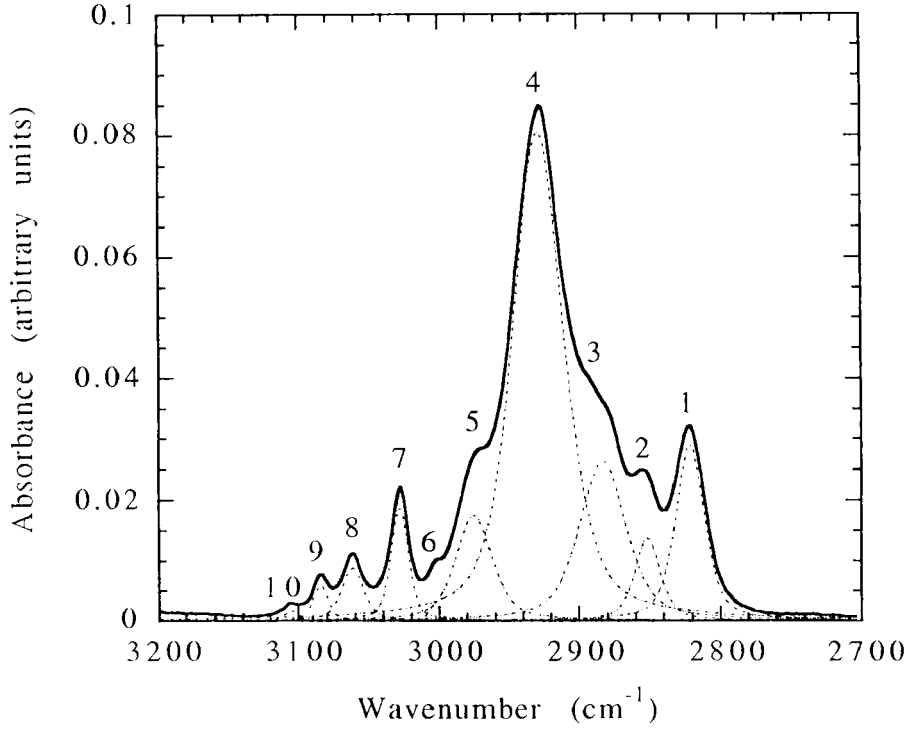

FIGURE 4 Deconvolution of the ATR-FTIR spectrum of a 50/50 w/w PS/PVME blend. The continuous line represents the original spectrum (see Figure 3), whereas the dashed lines are the deconvoluted peaks using 50% Lorentzian and 50% Gaussian distributions. The peak frequencies 1 through 10 are 2820, 2850, 2880, 2930, 2975, 3000, 3030, 3060, 3085, and 3105 cm^{-1}, respectively.

PS, a calibration curve was required. Blends of PS and PVME with known composition ranging from 10% to 90% PS by weight were cast on ZnSe crystal from a 1% solution in toluene at 250 rpm. The area under the peaks was determined by deconvoluting the original spectrum. The area of the PVME band at 2820 cm^{-1} and the PS bands at 2850 and 3030 cm^{-1} were used to calculate the relative absorption of PVME and PS.

Figure 5 shows the time evolution of the ATR-FTIR spectrum for interdiffusion in the PS/PVME pair at 65°C. The absorbance scale corresponds to the spectrum at zero interdiffusion time. The other spectra were shifted by 0.05 absorbance units for visual clarity. As interdiffusion proceeds, the PVME band at 2820 cm^{-1} increases with time and the PS bands at 2850 and 3030 cm^{-1} decrease with time. The spectra were deconvoluted, the relative absorption of PVME as a function of time was calculated, and the molar fraction of PVME was obtained from the calibration curve.

Figure 6 shows the increase in the PVME mole fraction as a function of time at 65, 75, and 95°C using a ZnSe crystal with PS and PVME film thicknesses of 500

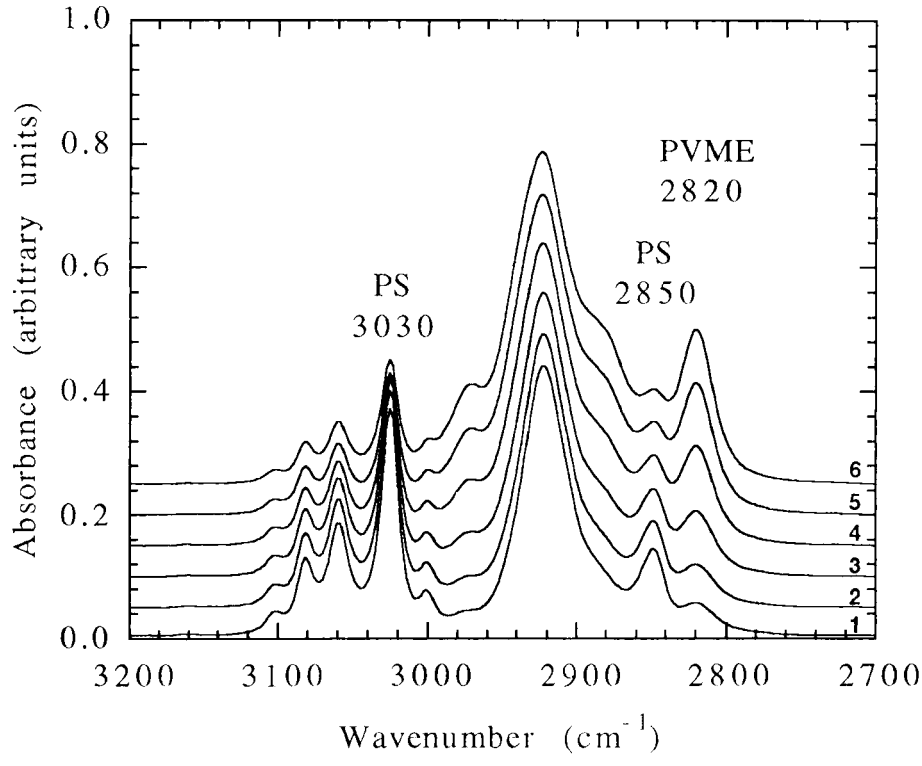

FIGURE 5 Time evolution of ATR-FTIR spectra for interdiffusion in a PS/PVME pair at 75°C. The PS and PVME molecular weights, $\overline{M}_n$, were 1.0×10^5 and 4.7×10^4 with polydispersity indices of 1.06 and 2.10, respectively. The PS film was spin cast on a ZnSe crystal at 250 rpm from a 5 wt% p-xylene solution. The PVME film was spin cast on the PS film at 250 rpm from a 10% isobutanol solution. The PS and PVME film thicknesses were 0.7 μm and 6.6 μm, respectively. The absorbance scale corresponds to spectrum 1 and the other spectra are shifted by 0.05 absorbance units. The spectra 1 through 6 correspond to 0, 5, 10, 15, 20, and 25 h of interdiffusion time, respectively.

nm and 6.6 μm, respectively. Figure 7 shows the increase in the PVME mole fraction as a function of time at 60, 70, and 80°C using a Ge crystal with PS and PVME film thicknesses of 90 nm and 3.1 μm, respectively. According to these figures, the rate of diffusion of PVME into the PS film increases as temperature increases.

Error analysis was carried out to determined the effect of the uncertainty in the values of the independent variables on the cumulative PVME concentration. These variables included refractive index of the polymers, wavelength of the infrared beam, PS and PVME film thickness, and the area of the deconvoluted peaks. The major sources of uncertainty included the PS film thickness and the area of the FTIR peaks.[23] Since the PVME film thickness was at least an order of magnitude greater than PS, a 20% uncertainty in the PVME film thickness resulted in less than 1% uncertainty in the PVME cumulative concentration.

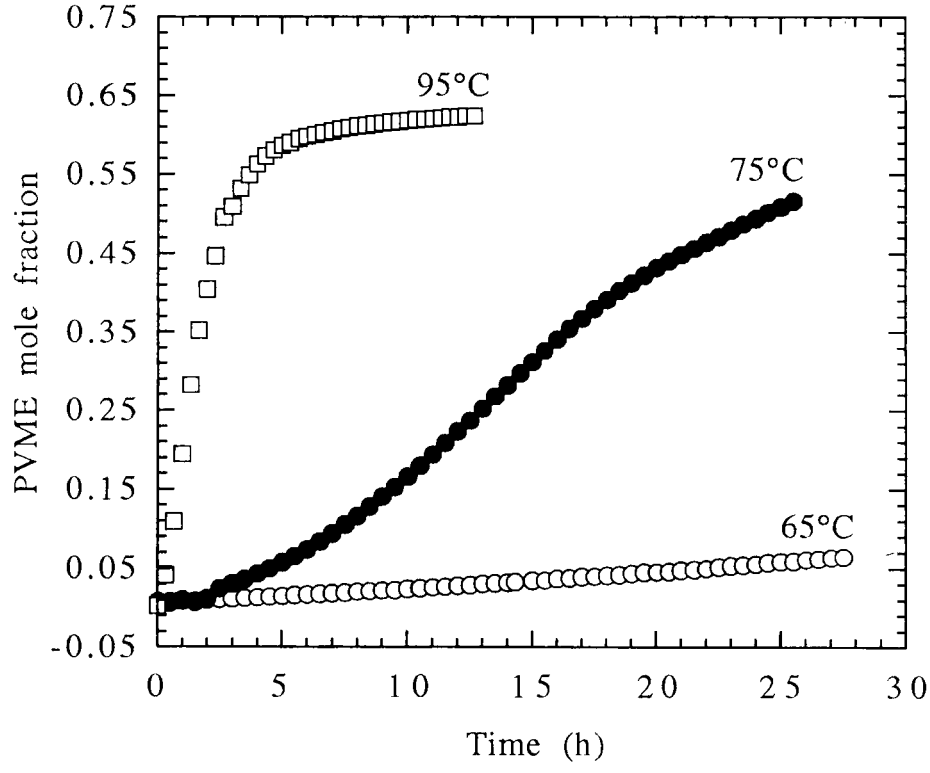

FIGURE 6 Mole fraction of PVME as a function of time during interdiffusion of PVME in PS at temperatures of 65°C (○), 75°C (●), and 95°C (□). The PS and PVME molecular weights, $\overline{M}_n$, were 1.0×10^5 and 4.7×10^4 with polydispersity indices of 1.06 and 2.10, respectively. The PS film was spin cast on a ZnSe crystal at 250 rpm from a 5 wt% p-xylene solution. The PVME film was spin cast on the PS film at 250 rpm from a 10 wt% isobutanol solution. The PS and PVME film thicknesses were 0.7 μm and 6.6 μm, respectively.

4. DISCUSSION

After intimate contact is established between two polymers with dissimilar properties, the faster-diffusing component swells the slower-diffusing component prior to interdiffusion across the interface. To confirm this swelling, PVME was contacted with crosslinked PS and dynamic mechanical analysis was used to follow the changes in the relaxation spectrum of the crosslinked PS/PVME bilayer before and after annealing. The thicknesses of the PS and PVME films were 0.6 mm and 25 μm, respectively.

Figures 8 and 9 show the shear storage modulus, G′, and the shear loss modulus, G″, for PS/PVME as a function of temperature, respectively. The lines in Figures 8 and 9 designated by 1, 2, and 3 correspond to the relaxation of crosslinked PS, crosslinked PS in contact with PVME after drying at 25°C for 24 h, and crosslinked PS in contact with PVME after annealing at 85°C for 5 days *in vacuo*. The sharp

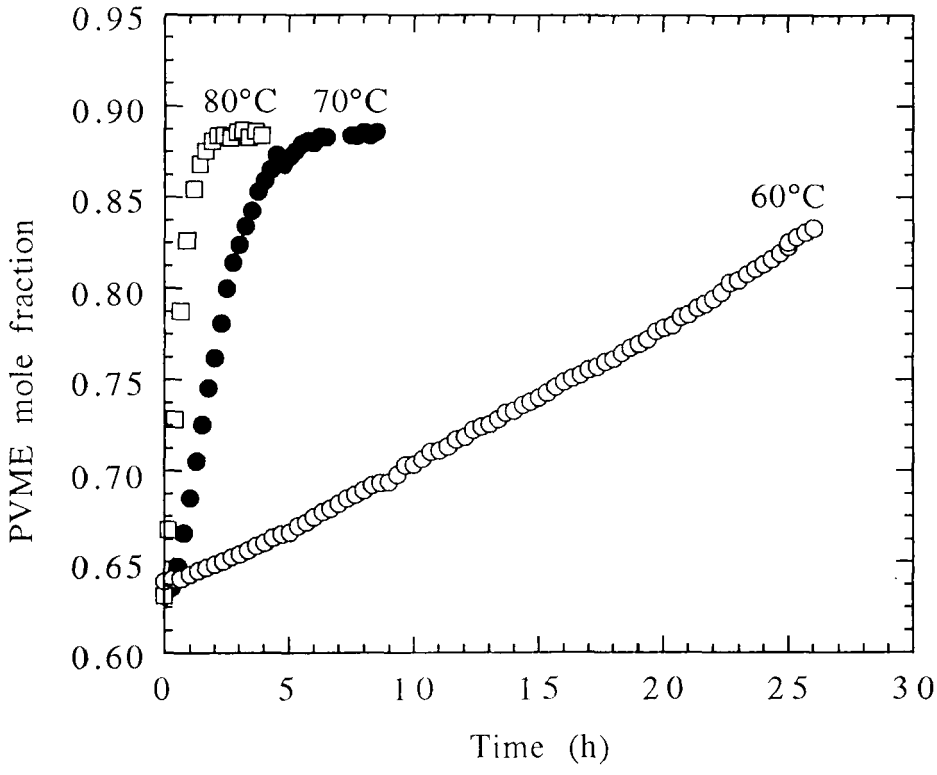

FIGURE 7 Mole fraction of PVME as a function of time during interdiffusion of PVME in PS at temperatures of 60°C (○), 70°C (●), and 80°C (□). The PS and PVME molecular weights, $\overline{M}_n$, were 1.0×10^5 and 4.7×10^4 with polydispersity indices of 1.06 and 2.10, respectively. The PS film was spin cast on a Ge crystal at 250 rpm from a 1 wt% p-xylene solution. The PVME film was spin cast on the PS film at 250 rpm from a 5 wt% isobutanol solution. The PS and PVME film thicknesses were 0.09 μm and 3.2 μm, respectively.

decrease in the storage modulus in Figure 8 and the relaxation peak in the loss modulus in Figure 9 close to 110°C correspond to the T_g of PS. The broad peak in the relaxation spectrum of crosslinked PS in contact with PVME before annealing, that is, line 2 in Figure 9, corresponds to the T_g of PVME. The relaxation spectrum of crosslinked PS (line 1) and crosslinked PS in contact with PVME before annealing (line 2) were essentially identical except for the relaxation peak of PVME centered around 0°C.

However, the relaxation spectrum of the crosslinked PS in contact with PVME after annealing (line 3) differs significantly from the other two spectra. In Figure 8, the glassy storage modulus of the PS/PVME bilayer decreased from 8.9×10^8 Pa before annealing to 5.6×10^8 Pa after annealing due to swelling of PS by PVME. The T_g of PS decreased by 5°C after annealing due to swelling of the PS matrix by PVME.

The swelling of PS by PVME below the T_g of PS was also confirmed in the shear loss spectrum of the annealed PS/PVME bilayer. In Figure 9, the relaxation peak

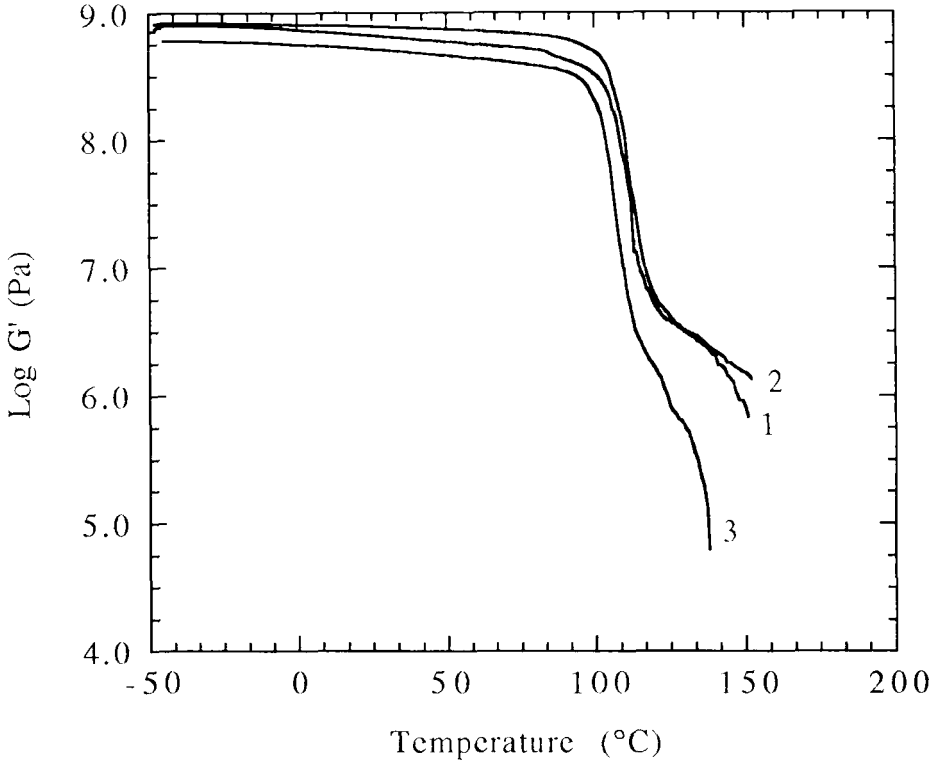

FIGURE 8 Temperature dependence of the shear storage modulus, G', for crosslinked PS (Curve 1), crosslinked PS in contact with PVME before annealing (Curve 2), and crosslinked PS in contact with PVME after annealing at 85°C for 5 days (Curve 3). The thicknesses of the crosslinked PS and the PVME were 0.6 mm and 25 μm, respectively.

of PVME centered at 0°C before annealing (line 2) changed to a broad relaxation ranging from −20 to 70°C after annealing (line 3) due to diffusion of PVME into the PS matrix. Also, the relaxation peak of PS centered at 104°C before annealing (line 2) shifted to 95°C after annealing (line 3). The DMA annealing experiments with crosslinked PS in contact with PVME clearly indicate that PVME swelled the glassy PS matrix due to the compatibility of PVME with PS, the low T_g of PVME, and the high mobility of the PVME chains.

The swelling of the PS matrix by PVME below the T_g of PS was shown[23] to be independent of the concentration gradient across the interface but dependent on the relaxation of the PS matrix. In other words, this swelling is a non-Fickian process limited by the relaxation time of the slow-diffusing component, PS. Therefore, the swelling process shown in Figures 6 and 7 is modeled using a zero-order relaxation process.

As the temperature was increased from 65 to 95°C, the rate of swelling of PS by PVME increased, as shown in Figure 6. At 65°C, the increase in concentration of PVME was linear in time corresponding to the initial stage of the swelling process.

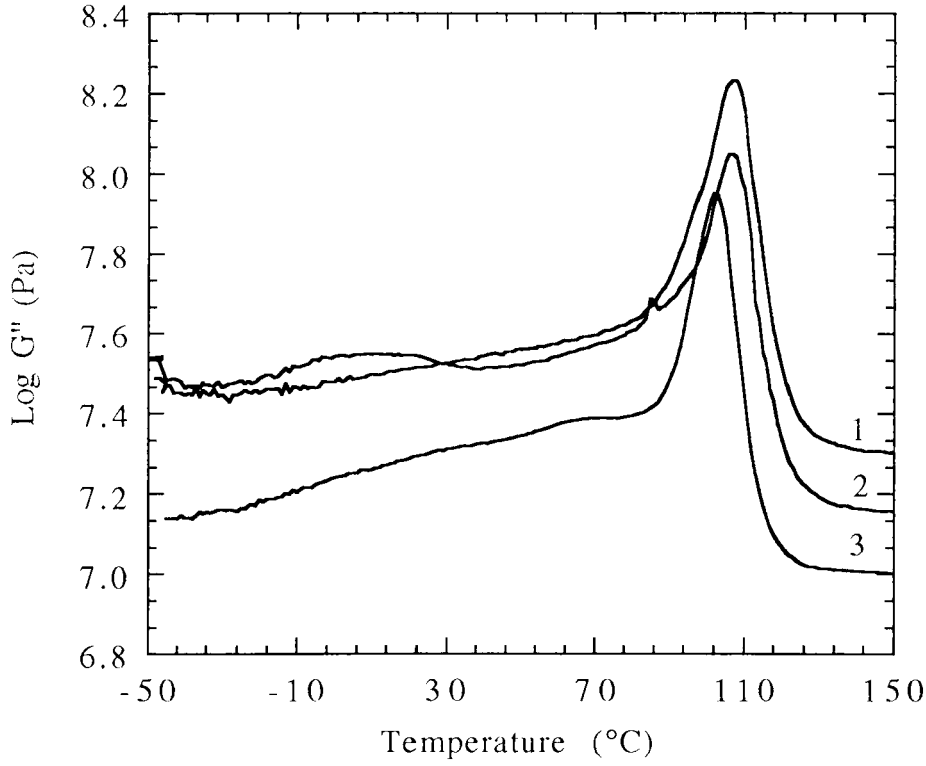

FIGURE 9 Temperature dependence of the shear loss modulus, G″, for crosslinked PS (Curve 1), crosslinked PS in contact with PVME before annealing (Curve 2), and crosslinked PS in contact with PVME after annealing at 85°C for 5 days (Curve 3). The thicknesses of the crosslinked PS and the PVME were 0.6 mm and 25 μm, respectively.

As temperature increased to 75°C, the increase in the PVME concentration with time was sigmoidal due to dramatic decrease of the relaxation time of the PS/PVME matrix with time. At 95°C, the increase in the PVME concentration was linear with time and reached a constant value when the PS/PVME interface reached the surface of the ATR crystal. In Figure 7, the initial PVME mole fraction was non-zero because the penetration depth of the IR beam in the polymer layer (114 nm for Ge crystal) was greater than the thickness of the PS layer which was 90 nm.

To understand this swelling behavior, we consider a PS layer with thickness, δ_1, and a PVME layer with thickness, δ_2, deposited on an ATR crystal, as shown in Figure 1. The swelling direction is along the z-axis which is perpendicular to the PS/PVME interface with the origin at the crystal/PS interface. The faster-diffusing component, PVME, diffuses into the slower-diffusing component, PS, and the original sharp interface moves into the slower moving component, PS, remaining as a sharp interface. The swelling process is characterized by an interface velocity, K_i, which defines how fast the interface moves into the PS layer. For constant K_i, the position of the interface can be written as:

$$z_i = \delta_1 - K_i t \tag{1}$$

where z_i is the position of the interface as a function of time.

The assumptions in Eq. (1) include: (i) the swelling of PS by PVME is one dimensional in the direction perpendicular to the interface; (ii) the diffusion process is independent of the concentration profile across the interface; (iii) there is no change of volume upon mixing PS and PVME; and (iv) there is no phase change which would alter the relaxation behavior of the PS matrix. These assumptions are valid because the bilayer film thickness is orders of magnitude smaller than the dimensions of the ATR crystal, the swelling process is non-Fickian, the excess volume of mixing for the PS/PVME pair is very small, and only the initial portion of the PVME cumulative concentration is used to calculate the interface velocity.

As the PVME swells the PS matrix with an interface velocity of K_i, it leaves behind a mixture corresponding to the equilibrium composition of PS/PVME films resulting in the following concentration profile:

$$c_{PV} = c_{PV}^{eq} \quad z_i \leq z < \delta_1 \quad t > 0 \tag{2}$$

$$c_{PV} = 0 \quad 0 \leq z < z_i \quad t > 0 \tag{3}$$

Here, c_{PV}^{eq} is the equilibrium concentration of PVME obtained from the experimental data at 95°C in Figure 6 and at 70 or 80°C in Figure 7, respectively. The relative intensity of the radiation as a function of distance away from the crystal surface is given by:

$$I_{rel} = e^{-z/d_p} \tag{4}$$

Here, I_{rel} is the IR intensity relative to the intensity at the interface and d_p is the penetration depth of the IR radiation in the PS layer. The penetration depth is defined as the depth at which the intensity of the radiation decreases to 1/e of its value at the crystal surface. According to Eq. (4), the intensity decreases exponentially away from the interface. The penetration depth of the IR radiation is a function of infrared frequency, refractive indices of the crystal and polymer, and the incident angle of the beam. The penetration depths for PS on Ge and ZnSe crystal with incident angle of 45° at 3000 cm^{-1} are 114 and 350 nm, respectively.

The exponential decrease of IR intensity within the penetration depth has to be considered in order to compare experimental results with the model predictions. For an interdiffusion time, t, the concentration of PVME, c_{PV}, at distance z from the crystal surface is multiplied by its corresponding relative intensity, I_{rel}, given by Eq. (4), and is integrated over the penetration depth of IR radiation inside the polymer layer. This process is repeated for each interdiffusion time to give the cumulative amount of PVME, Q_{PV}, inside the penetration depth *versus* time:

$$Q_{PV} = \frac{\int_0^\infty c_{PV}(z,t)\, I_{rel}(z)\, dz}{\int_0^\infty I_{rel}(z)\, dz} \tag{5}$$

Substituting for c_{PV} from Eqs. (2) and (3) in Eq. (5) and integrating results in the following relation between the cumulative concentration of PVME and time:

$$Q_{PV} = c_{PV}^{eq} \exp\left[\frac{-2(\delta_1 - K_i t)}{d_p}\right] \tag{6}$$

The derivative of cumulative concentration with respect to time as time approaches zero represents the rate of PVME diffusion:

$$\lim_{t \to 0} \frac{dQ_{PV}}{dt} = c_{PV}^{eq} \left(\frac{2K_i}{d_p}\right) e^{-2\delta_1/d_p} \tag{7}$$

As expected, this rate is directly proportional to the interfacial velocity, K_i. From the slope of the PVME cumulative concentration *versus* time (Fig. 10) the interfacial velocity could be calculated. These data are reported in the third column of Table I.

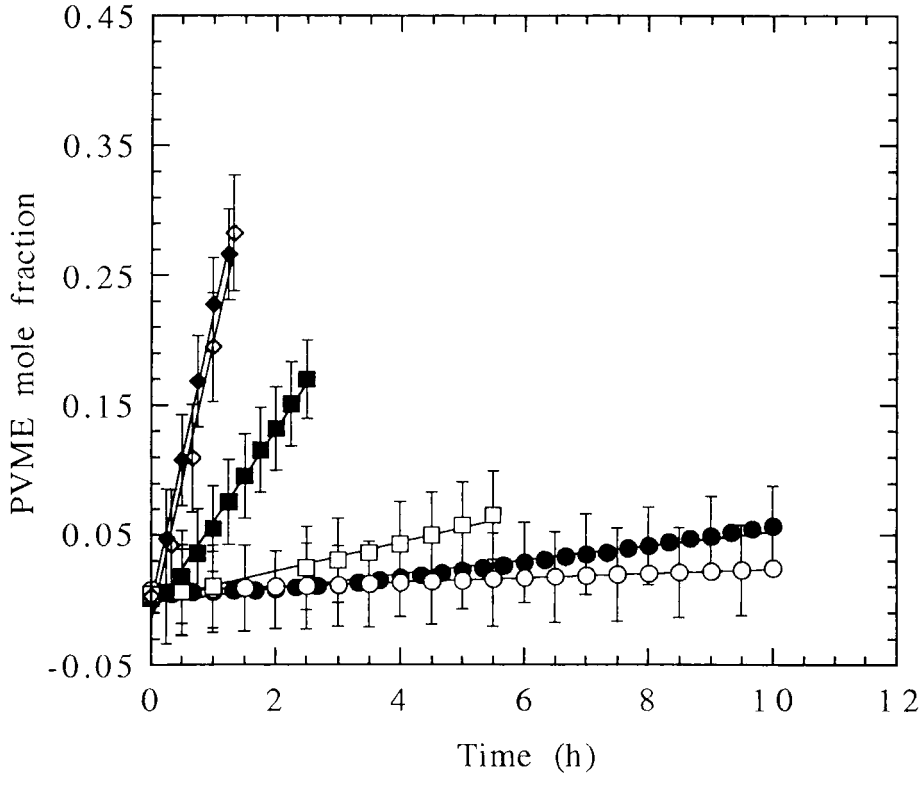

FIGURE 10 Early portion of the cumulative concentration of PVME as a function of time during diffusion of PVME in PS at temperatures of 60°C (●) on Ge, 65°C (○) on ZnSe, 70°C (□) on Ge, 75°C (■) on ZnSe, 80°C (◇) on Ge, 95°C (◆) on ZnSe. The PS and PVME molecular weights, $\overline{M}_n$, were 1.0×10^5 and 4.7×10^4 with polydispersity indices of 1.06 and 2.10, respectively.

TABLE I
Temperature dependence of the interfacial velocity, K_i, relaxation time, τ, and interfacial thickness, δ_i, for PS/PVME systems

Diffusion temperature, T (°C)	Slope of PVME mole fraction *vs.* time $\times 10^3$ (s^{-1})	Interfacial velocity, $K_i \times 10^{10}$ (cm/s)	Relaxation time, τ (s)	Interfacial thickness, δ_i (nm)
60	6.36 ± 0.35	1.12 ± 0.06	8480 ± 463	4.0 ± 0.2
65	1.72 ± 0.19	4.77 ± 0.52	1990 ± 219	17.2 ± 1.9
70	68.0 ± 1.70	12.0 ± 0.30	792 ± 20	43.2 ± 1.1
75	8.81 ± 0.22	24.4 ± 0.60	389 ± 9	87.8 ± 2.2
80	199 ± 5	35.0 ± 0.90	271 ± 7	126 ± 3
95	204 ± 5	564 ± 14	16.8 ± 0.4	2030 ± 51

To examine the importance of relaxation on interdiffusion, the limiting relaxation time, τ, for swelling of PS by PVME was calculated using the following relationship:

$$\tau = \frac{r_g}{K_i} \tag{8}$$

where r_g is the radius of gyration of a polymer chain. The radius of gyration of a PS chain with $\overline{M_n}$ of 1.0×10^5 is 9.5 nm. The limiting relaxation times at 60, 65, 70, 75, 80, and 95°C are 8480, 1990, 792, 389, 271, and 16.8 s, respectively. An alternative determination of the relaxation time can be made from the relaxation time of a polymer chain in the melt:[27,28]

$$\tau_{rep} = \left(\frac{48}{5}\right)\left(\frac{L^2}{\pi^2 RT}\right)\left(\frac{M_e^2}{\rho\, b^2\, M_o}\right)\eta_o \tag{9}$$

Here, τ_{rep} is the relaxation time of a chain using reptation theory, L is the contour length of a polymer chain, R is the gas constant, T is temperature, M_e is the entanglement molecular weight, M_o is the repeating unit molecular weight, ρ is the polymer density, b is the statistical segment length, and η_o is the zero shear viscosity of the polymer which is temperature dependent. Knowing the relaxation time and the zero shear viscosity at one temperature, the relaxation time at other temperatures can be estimated. The relaxation time of PVME with $\overline{M_w}$ of 5.5×10^4 at 160°C is 0.03 s.[29] The zero shear viscosity of PVME with $\overline{M_w}$ of 1.05×10^5 at 160°C is 1.78×10^3 kg/m s.[30] The Williams, Landel, and Ferry (WLF) equation was used to estimate the zero shear viscosity of PVME at temperatures other than 160°C.

At 95°C, corresponding to 5°C below the T_g of PS, the estimated PVME relaxation time is 0.4 s which is 40 times smaller than the experimental relaxation time. As temperature decreases, the estimated PVME relaxation time becomes even smaller than the experimental relaxation time. At 60°C, corresponding to 40°C below the T_g of PS, the estimated relaxation time is 6 s which is three orders of magnitude smaller than the experimental relaxation time. This clearly indicates that the rate of swelling of the PS matrix by PVME is controlled by the relaxation time of the slow-diffusing polymer chains, *i.e.* by PS.

The experimentally-determined relaxation times can be used to determine the

activation energy for relaxation of a PS chain which is the controlled step in the swelling of PS by PVME. The Arrhenius equation is used to describe the temperature dependence of the relaxation time given by:

$$\tau = \tau_o \exp\left[\frac{E_{rel}}{R}\left(\frac{1}{T} - \frac{1}{T_o}\right)\right] \tag{10}$$

Here, τ_o is the relaxation time at a reference temperature T_o and E_{rel} is the activation energy for the relaxation. The least squares best fit of these data (Fig. 11) gave a slope of $2.06 \pm 0.13 \times 10^4$ K corresponding to an activation energy of 40.9 ± 2.6 kcal/mol. This activation energy is in good agreement with the values reported in the literature[31,32] for the β relaxation of PS which is of the order of 35–40 kcal/mol. The β relaxation of PS is attributed to the onset of flow. The last column of Table I gives the interfacial thickness of the PS/PVME bilayer after annealing for one hour at different temperatures. The interfacial thickness of the PS/PVME bilayer at 60, 65, 70, 75, 80, and 95°C are 4.0, 17.2, 43.2, 87.8, 126, and 2030 nm, respectively.

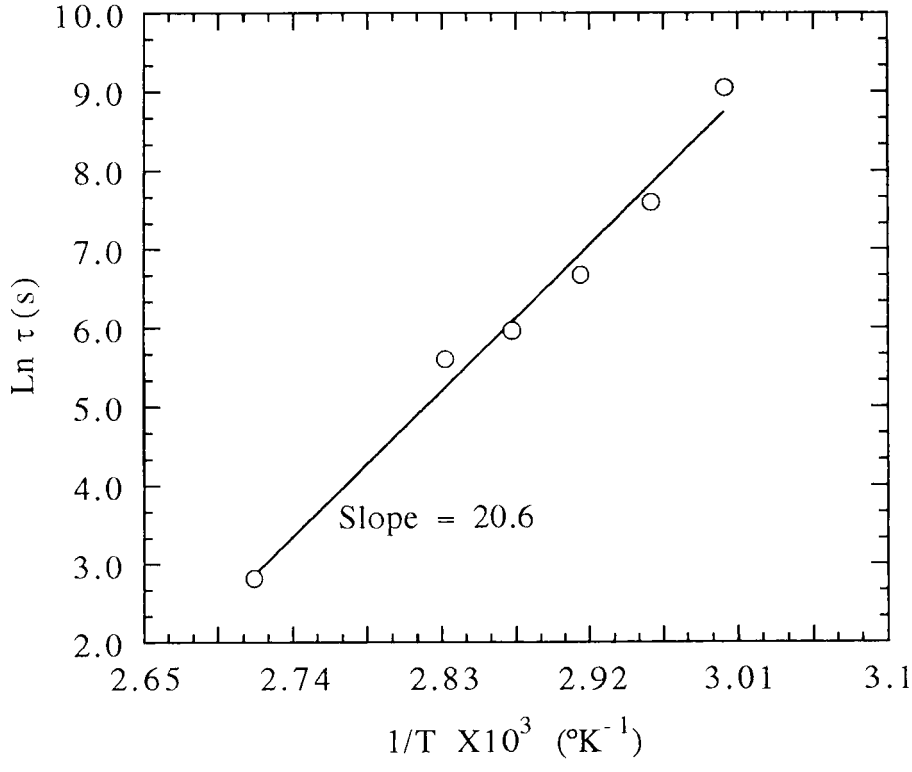

FIGURE 11 Plot of logarithm of relaxation time *versus* inverse temperature to determine the activation energy for swelling of the PS matrix by PVME. The PS and PVME molecular weights, $\overline{M}_n$, were 1.0×10^5 and 4.7×10^4 with polydispersity indices of 1.06 and 2.10, respectively.

5. CONCLUSIONS

When PS below its glass transition temperature comes in contact with PVME, the PVME swells the glassy PS. This swelling was confirmed by dynamic mechanical analysis (DMA) using crosslinked PS in contact with PVME. The DMA results indicated that PVME swells the crosslinked PS below its T_g. The swelling was followed quantitatively using ATR-FTIR spectroscopy. The swelling process was characterized by an interfacial velocity as the PVME swelled the glassy PS matrix. The relaxation time for the swelling was determined from the interface velocity as a function of temperature and the results indicated that the swelling process was controlled by the relaxation time of the slow-diffusing component, PS. The relaxation time ranged from 8480 s at 60°C to 16.8 s at 95°C.

The activation energy for the relaxation of the PS matrix was determined using the Arrhenius equation and it was found to be 40.9 ± 2.6 kcal/mol. This activation energy is in good agreement with the values reported in the literature for the β relaxation of PS which is in the range of 35–40 kcal/mol. It is interesting to note that the literature activation energy determined from dynamic mechanical experiments corresponds surprisingly well to the activation energy obtained from a microscopic analysis such as polymer-polymer interdiffusion.

Acknowledgments

This research was the winner of a 1992 Graduate Research Award by The Adhesion Society and was presented in preliminary form at the Annual Meeting of the Society in Hilton Head, SC, in February, 1992. This work was supported by a National Institutes of Health (NIH) grant No. GM45027, whereas the ATR-FTIR spectrometer was supported by a National Science Foundation (NSF) grant No. CTS-90-07141.

References

1. K. Jud, H. H. Kausch and J. G. Williams, *J. Mater. Sci.* **16,** 204 (1981).
2. K. L. Saenger, H. M. Tong and R. D. Haynes, *J. Polym. Sci. Polym. Lett.* **27,** 235 (1989).
3. C. Creton, E. J. Kramer, C. Y. Hul and H. R. Brown, *Macromolecules* **25,** 3075 (1992).
4. H. W. Kammer, *Acta Polymerica* **34,** 112 (1983).
5. W. H. Pritchart, *Aspects of Adhesion* **6,** 12 (1971).
6. W. D. Bascom, *Adv. Polym. Sci.* **85,** 89 (1988).
7. W. Possart, *Int. J. Adhes. Adhes.* **8,** 77 (1988).
8. J. G. Lertola and J. M. Schultz, *J. Appl. Polym. Sci.* **40,** 113 (1990).
9. S. S. Voyutskii, *J. Adhesion* **3,** 69 (1971).
10. J. Comyn, in *Polymer Permeability,* J. Comyn, Ed. (Elsevier, Amsterdam, 1985), p. 177.
11. E. H. Andrews, *J. Polym. Sci. Polym. Symp.* **72,** 295 (1985).
12. A. N. Gent and C. W. Lin, *J. Adhesion* **32,** 113 (1990).
13. K. H. Dai, E. J. Kramer and K. R. Shull, *Macromolecules* **25,** 220 (1992).
14. P. G. de Gennes, *C. R. Acad. Sci. Paris, Serie II* **292,** 1505 (1981).
15. M. S. High, P. C. Painter and M. M. Coleman, *Macromolecules* **25,** 797 (1992).
16. C. M. Roland and G. G. A. Bohm, *Macromolecules* **18,** 1310 (1985).
17. J. Sokolov *et al., Polym. Prepr.* **31**(2), 79 (1990).
18. P. J. Mills, P. F. Green, C. J. Palmstrom, J. W. Mayer and E. J. Kramer, *Appl. Phys. Lett.* **45,** 957 (1984).
19. E. Jabbari and N. A. Peppas, *Polym. Bull.* **27,** 305 (1991).
20. P. P. Hong, F. G. Boerio, S. J. Clarson and S. D. Smith, *Macromolecules* **24,** 4770 (1991).
21. J. Klein and B. J. Briscoe, *Polymer* **17,** 481 (1976).
22. B. B. Sauer and D. J. Walsh, *Macromolecules* **24,** 5948 (1991).

23. E. Jabbari and N. A. Peppas, *Macromolecules* **26,** 2175 (1993).
24. N. J. Harrick, *Internal Reflection Spectroscopy* (Wiley, New York, 1967), p. 27.
25. H. Park, E. M. Pearce and T. K. Kwei, *Macromolecules* **23,** 434 (1990).
26. H. Yang, M. Shibayama, R. S. Stein, N. Shimizu and T. Hashimoto, *Macromolecules* **19,** 1667 (1986).
27. W. W. Greassley, *J. Polym. Sci. Polym. Phys.* **18,** 27 (1980).
28. E. Jabbari and N. A. Peppas, *Polymer,* in press.
29. A. Ajji, L. Choplin and R. E. Prud'Homme, *J. Polym. Sci. Polym. Phys.* **26,** 2279 (1988).
30. Y. Takahashi, H. Suzuki, Y. Nakagawa, M. Yamaguchi and I. Noda, *Polym. J.* **23,** 1333 (1991).
31. N. G. McCrum, B. E. Read and G. Williams, *Anelastic and Dielectric Effects in Polymeric Solids* (Wiley, New York, 1967), p. 411.
32. K. H. Illers and E. Jenckel, *J. Polym. Sci.* **41,** 528 (1959).